

HIGH RESOLUTION DEMOIRÉ NETWORK

ABSTRACT

Photographing LCD screens for recording information has become a prevalent behavior, moiré artifact will appear in screen-shotted pictures with different color and shape. In order to remove such artifacts, previous work mainly used multi-scale framework to identify the complex frequencies of moiré, but the relationship of different scale used to be ignored. In this paper, we proposed a novel High-Resolution Demoiré Network(HRDN) to fully explore the relationship between feature maps with different resolutions. It consists of three main components: parallel high-resolution network, continuously information exchange modules and final feature fusion layer. Extensive experiments on benchmark dataset demonstrate that our method outperform the state-of-art both in quantity and quality, and the psnr of demoiré images restored by HRDN reached 28.47, which is 0.72 higher than MopNet [1] from ICCV2019.

Index Terms— Demoiré, High-Resolution Network, Image Processing, Compute Photography

1. INTRODUCTION

Taking a picture from LCD screen is a common scene in our daily life, for example, photograph to save information from slides on a public report or a class, we call such images as screen-shot images/pictures. But there is a fatal problem in the screen-shot picture—moiré patterns, which is shown in Figure 1, moiré pattern is an unpleasant artifact on most screen-shot image, it severely degrades the image quality and therefore damages the information we wanna store.

Moiré patterns is a manifestation of the phenomenon of beats, the phenomenon of beats can be expressed as follows: when two waves with similar frequencies are combined, the frequencies of combined wave is equal to the difference between the two original frequencies. The moiré patterns appear more clearly when we use a camera or smartphone to shoot against the LCD screen, due to the analog signal interference between the LCD screen and Color Filter Array(CFA) of camera sensor, usually their frequencies are similar, the misalignment between them causes the moiré.

Demoiréing can be regarded as an image restoration problem, from on point of view, the goal of image restoration generally is to remove noise and restore details. From another point of view, image demoiré is aims to remove moiré

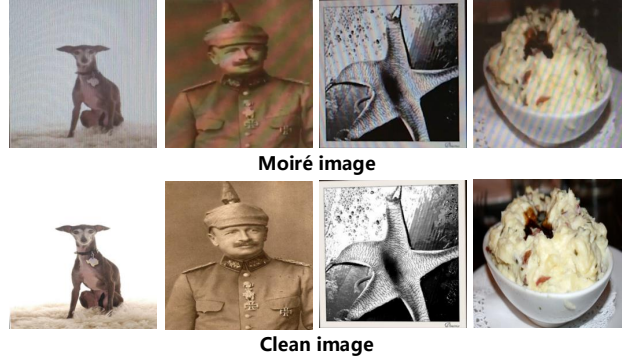


Fig. 1. Above represent contaminate images with moiré pattern, below represent clean images

pattern and restore textures and colors. But there are several difference between the demoiré task and traditional image restoration tasks such as denoising, deraining, super-resolution. The most significant difference is a moiré pattern can span over a wide range of frequencies, it exists from low frequencies to high frequencies within contaminate images, but traditional image restoration methods can only process single-frequency artifacts. Traditional moiré pattern removal algorithms mainly solve simple moiré pattern appears in highly textured image such as cloth and building. Wei et al. [2] used a median-Gaussian filtering method to remove moiré in X-ray microscopy images, Liu et al. [3] proposed a low-rank and sparse matrix decomposition method to separate moiré pattern and texture. They are little effects and cannot solve complex moiré appearing in the screen-shot image. Recently convolutional neural network(CNN) has proven great success in low level vision task, some deep-learning based models have been developed to tackle the screen-shot moiré image, Sun et al. [4] implement a multi-resolution fully convolutional neural network to model moiré pattern by training from a large-scale dataset, but their network is so simple that has limited effects. Gao et al. [5] improved Sun's approach by exploring the relationships among features with multiple resolutions, they called Feature Enhance Branch(FEB), but such FEB didn't fully explore the relationship between different branches, so they have not ideal performance. He et al. [1] propose a Moiré pattern Removal Neural Network(MopNet), they use the integration of three specially designed network to achieve highest psnr so far.

In this paper, we propose a novel High-Resolution Demoiré Network(HRDN) for screen-shot image demoiré. The network is a parallel multi-scale architecture with residual blocks. Different from encoder-decoder architecture like U-net [6] and previous multi-scale network like [4, 5], to fully take advantage of the feature map from multiple scale, we use Information Exchange Modules(IEM) and Final Feature Fusion Layer(FFF) to continuously exchange information throughout the network. We also pay attention to the edge intensities by use edge enhanced loss function during the training stage. Our contributions can be summarizing as follows:

- In view of the multi-frequencies characteristics of moiré pattern. We propose a novel High-Resolution Demoiré Network(HRDN), which can maintain full resolution while processing the lower resolution, and handle the different frequency in different scale.
- The relationship between feature maps from different scale should be explored by continuously exchange information. So we propose Information Exchange Module(IEM) and Final Feature Fusion Layer(FFF) to fully fuse the feature from low level to high level, and from high level feature to low level feature too.
- Pixel-wise loss function results in over-smoothing, which loses details and edge texture. We implement the Edge Enhanced Loss to enhance the edge and preserve the detail.
- By extensive experiments on the Moire Image Benchmark, we demonstrate that the proposed HRDN can remove moiré pattern efficiently and outperform the state-of-arts.

2. RELATED WORK

2.1. Image restoration

Image demoiréing can be regarded as another image restoration task, recently, several learning-based image restoration methods have achieved great success both quantitatively and in qualitatively. Common image restoration researchers dedicate to tasks such as image denoising, deblurring, deraining and super-resolution. But in contrast, few researchers pay their attention on demoiréing.

In facts, this task is more difficult than others, since common image restoration just only process high frequency or static artifacts, for example, image denoising focuses on eliminating high frequency noise, the goal of image deraining is also eliminating raindrops which appear as high frequency noise in the image, and super-resolution task aims to reconstruct the texture details of high resolution image which is also high frequency. The moiré patterns for image demoiréing exist at both high frequency and low frequency and appear as dynamic artifacts. The dynamic characteristics are reflected not only in different images, but also in different location of same image.

2.2. Image demoiréing

2.2.1. Traditional methods

Traditional demoiréing approaches mainly model the well-patterned textures, Wei et al. [2] used a median-Gaussian filtering method to remove moiré in X-ray microscopy images. Liu et al. [3] proposed a low-rank and sparse matrix decomposition method to separate moiré pattern and texture. Their method can only handle the moiré patterns appearing in textured images, it is simpler than screen-shot moiré pattern. Yang et al. [7] proposed a layer decomposition based on polyphase components(LDPC) to remove the screen-shot moiré. This method can remove some small moiré pattern, but it can not handle larger artifacts, meanwhile, the algorithm has high time complexity.

2.2.2. Deep learning based methods

Deep learning has achieved impressive results in many fields, computer vision and image restoration also benefit from convolutional neural networks. There are several deep learning based image demoiré methods during these years. Sun et al. [4] proposed a multi-resolution convolutional neural network to model the multi frequencies moiré pattern. They also created a large dataset which contain 135,000 pairs of contaminated and clean images from ImageNet [8]. As far as we know, this is by far the first and only true moiré image dataset, so it is important for developing demoiré methods, they called it Moire Photo Benchmark. He et al. [1] propose a Moiré pattern Removal Neural Network(MopNet), all core components of MopNet are specially designed for unique properties of moiré patterns, including the multi-scale feature aggregation, the channel-wise target edge predictor, the attribute-aware classifiers. But their networks are really complex, since they must pretrained the other two additional network for edge prediction and moiré' attribution classification. Liu et al. [9] proposed Deep Convolutional Neural Network(DCNN) which consists of a coarse-scale network and a fine-scale network, they integrate idea of generative adversarial network(GAN) in their architecture. In addition, they also proposed a method for synthesizing moiré images. However, their method only process the low-resolution image and reconstruct to original resolution, moiré pattern can span over a wide range of frequencies, so their method are not able to remove all the moiré pattern.

We propose a novel High-Resolution Demoiré Network(HRDN) to tackle aforementioned problem. We use two vital concepts: multi-scale and information exchange. Based on these, we proposed a parallel high-resolution network which can maintain every resolution throughout the whole network. Information Exchange Module(IEM) and Final Fusion Layer(FL) aims at fusing information from different resolutions. Details of our network are in the next section.

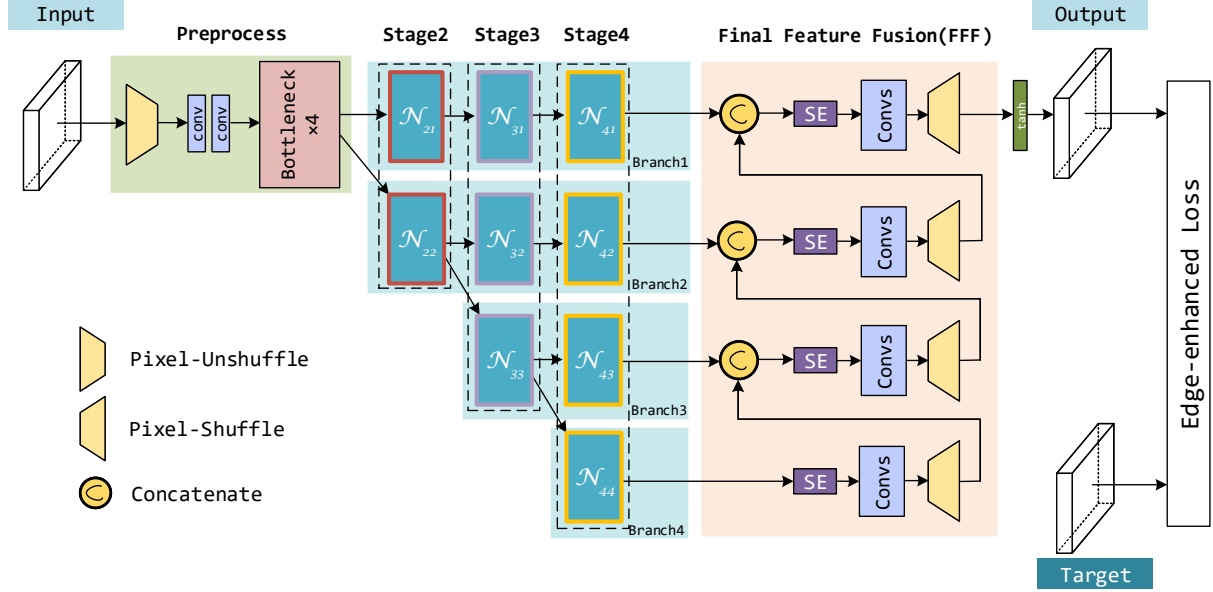


Fig. 2. Architecture of High Resolution Demoiré Network, it consists of three main parts: left is preprocess, middle is backbone with several stages, and right is final feature fusion, at last of network is edge-enhanced loss function.

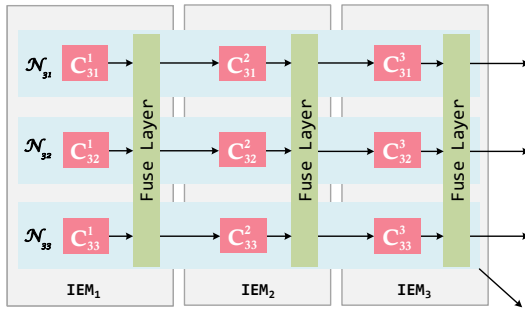


Fig. 3. The example of stage3 with three IEMs, N represents a subnetwork, C represents an IEM of subnetwork in one IEM.

3. METHOD

Screen-shot image demoiré aims to remove moiré pattern from contaminate screen-shot images, we define the problem as follow: Given an input image X contaminated by moiré pattern, excepted output Y of model $f(x)$ is a clean image that has none moiré pattern. Furthermore, the difference between output Y and groudtruth \hat{Y} should be as small as possible.

3.1. High-resolution demoiré network

Inspired by the HRNet in the field of pose estimation of Sun et al. [10] at CVPR 2019. We design our High-Resolution Demoiré Network (HRDN) that is depicted in Figure 2. The backbone of HRDN has two vital schemes: parallel multi-resolution architecture and continuously information exchange. Both two schemes aim to better tackle the multi-

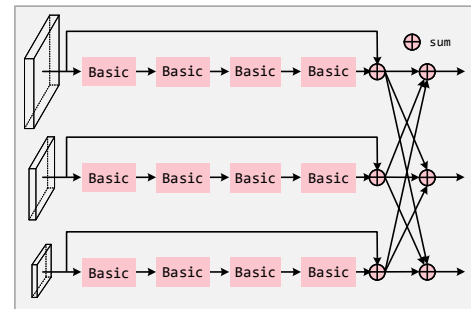


Fig. 4. An Information Exchange Module, the basic-block is proposed by ResNet [11], we add inter-block shortcuts for global residuals, the fuse layer can be describe as summing features from different scale.

frequencies and dynamic features of moiré pattern. We will detail in below.

A series of computer vision task need the output of model with original resolution as same as input, so several networks were developed to address this issue, such as FCN [12], U-net [6], Hourglass [13], Cascaded pyramid networks [14], VDSR [15], etc. However, these networks always downsample the input images to the low-resolution feature maps first, and then reconstruct the high-resolution results from the small feature map. We believe that some information would be lost during the cascade high-to-low-to-high process. To preserve these information, we do the similar operations when down-sample, instead of discard the high resolution feature maps, we maintain the high resolution by simultaneous processing both high resolution and low resolution.

Table 1. Preprocess Block parameter settings

Type	Kernel	Stride	Pad	Outputs
PixelShuffle	2	-	-	(128, 128, 12)
Conv	3x3	1	1	(128, 128, 64)
Conv	3x3	1	1	(128, 128, 64)
BottleNeck	3x3	1	1	(128, 128, 256)
BottleNeck	3x3	1	1	(128, 128, 256)
BottleNeck	3x3	1	1	(128, 128, 256)
BottleNeck	3x3	1	1	(128, 128, 256)

We follow the principle proposed by Sun et al. [4], to tackle the multiple frequencies characteristics of moiré pattern, the parallel multi-resolution architecture should be used. Thus HRDN introduce R parallel branches with full, $\frac{1}{2}, \frac{1}{4}, \frac{1}{8}, \dots$ resolutions, each branch can vertical split into subnetworks within S stages, which can be found in the middle blue part of Figure 2. Let \mathcal{N}_{sr} be the subnetwork in the s th stage and r represent r th branch (the resolution is $\frac{1}{2^{r-1}}$ of the first branch), so the backbone of HRDN can be describe as follows ($r = 4$):

$$\begin{aligned}
Preprocess &\rightarrow \mathcal{N}_{21} \rightarrow \mathcal{N}_{31} \rightarrow \mathcal{N}_{41} \\
&\searrow \mathcal{N}_{22} \rightarrow \mathcal{N}_{32} \rightarrow \mathcal{N}_{42} \\
&\quad \searrow \mathcal{N}_{33} \rightarrow \mathcal{N}_{43} \\
&\quad \quad \searrow \mathcal{N}_{44}
\end{aligned} \quad (1)$$

We start from an input image has 3 dimension (W, H, 3), transfer the input to preprocessing stage which can be found in Figure 2. Limited by the GPU memory, we first use pixel-shuffle block [16] with scale factor=2 to downsample image size into (W/2, H/2, 12) without losing pixel value. 2 conv-bn-relu layer followed by 4 bottleneck blocks [11] are used behind. Then gradually add lower resolution subnetworks using downsample meanwhile the higher resolution is keeping forward propagating. The subnetworks include M Information Exchange Modules will detail in next paragraph.

3.2. Information exchange module

We use Information Exchange Module(IEM) like HR-Net’s [10] to perform parallel convolution operation and fuse multiple resolution feature map at every stage. As shown in Figure 3, each stage contains M IEMs, Figure 4 shows the specific structure of an information exchange module. There are several branches in IEM, and each branch consists of 4 residual basic blocks proposed by ResNet [11], besides intra-block local residuals, we add inter-block global residuals for better learning the moiré pattern. A fusion layer used behind these residual block to fuse several feature maps from different branches. The relationships of each branch can be fully explored using such modules.

Table 2. Final Feature Fusion parameter settings

Branch	Type	Outputs
1	Concat	(128, 128, 19)
	SE	(128, 128, 19)
	Conv3x3	(128, 128, 12)
	PixelUnshuffle	(256, 256, 3)
2	Concat	(64, 64, 35)
	SE	(64, 64, 35)
	Conv3x3	(64, 64, 16)
	Conv3x3	(64, 64, 12)
3	Concat	(32, 32, 67)
	SE	(32, 32, 67)
	Conv3x3	(32, 32, 32)
	Conv3x3	(32, 32, 16)
4	Concat	(16, 16, 128)
	SE	(16, 16, 128)
	Conv3x3	(16, 16, 64)
	Conv3x3	(16, 16, 32)
	Conv3x3	(16, 16, 16)
	Conv3x3	(16, 16, 12)
	PixelUnshuffle	(32, 32, 3)

3.3. Final Feature Fusion and edge-enhanced loss

Final Feature Fusion(FFF) further combine the outputs from previous modules. In our HRDN, networks have R branches, the corresponding outputs have full, $\frac{1}{2}, \frac{1}{4}, \frac{1}{8}, \dots$ resolutions of first branch. As shown in Figure 2, we implement FFF down-to-top. We use a SE block [17] to perform channel-wise attention on each branch’s outputs first. Then using a series of 3x3 Conv layers reduce the number of channels to 12 while keeping the feature maps’ size unchanged. Followed by a pixel-unshuffle operation to scale up the size of feature maps twice with the number of channels is 3. Pixel-unshuffle can be seen as the reverse version of pixel-shuffle. At last, the feature maps enlarged from pixel-unshuffle are concatenated to higher resolution feature. Because of the imbalance of the channel after concatenating, we adopt the SE block to alleviate this problem. So the final outputs of HRDN can be expressed as:

$$Y = Tanh(f_1\{g[y_1, f_2(g(y_2, \dots))]\}) \quad (2)$$

where y_i is the outputs of branch i , and Y is the output demoiré image, f_i represents SE-Conv3x3-PixelUnshuffle operation. The function $g(\cdot, \cdot)$ is concatenating two feature maps at channel-wise. $Tanh()$ is a activate function that normalize the outputs to [-1, 1].

Finally, we define a edge-enhanced loss function to preserve the edge detail of demoiré image, it can be expressed as

follow:

$$\mathcal{L} = \alpha * CLoss + (1 - \alpha) * SLoss \quad (3)$$

$CLoss$ is L1 Charbonnier Loss and $SLoss$ is L1 Sobel Loss, their definitions as follow:

$$CLoss = \frac{1}{N} \sum_{i=1}^N \sqrt{(\hat{Y} - Y)^2 - \epsilon^2} \quad (4)$$

$$SLoss = \frac{1}{N} \sum_{i=1}^N \sqrt{(Sobel(\hat{Y}) - Sobel(Y))^2}$$

where N represents the batch size, \hat{Y} and Y denote the outputs demoiré image of HRDN and ground truth clean image without moiré pattern, respectively. The hyperparameter $\epsilon = 0.001$, and α is an adjustable parameter during the training.

3.4. Network instantiation

Our HRDN contains 4 branches whose resolution is gradually decreased to a half and accordingly the depth (number of channels) is increased to the double. We vertical split the network into 4 stage. The first stage also called preprocess, we will detail the preprocess block at Table 1.

The 2nd, 3rd, 4th stages contain 1, 4, 3 IMEs, respectively. One IME include 4 residual basic blocks proposed by He et al. [11]. We additionally implement the inter-block global residuals as Figure 4. Each branch has its depth C , and C is kept constant throughout the backbone of network, limited by GPU memory, we set the C of 4 branches are 16, 32, 64, 128.

Above Final Feature Fusion is used after backbone, The details of FFF can be found in Table 2. Every conv layer we used is 3×3 with stride 1 and padding 1 followed by BN and ReLU.

4. EXPERIMENTS

4.1. Training details and datasets

We use the Moiré Photo Benchmark created by Sun et al. [4]. They used 3 smartphones shooting against 3 LCD screens, and collect the moiré image from ImageNet [8]. The whole benchmark consist of 135,000 screen-shot images with moiré artifacts, each contaminate image has corresponding clean image without artifacts, which directly obtained from ImageNet. We set the training set and testing set as same as Sun, 90% are used to train, 10% are used to test. The details of datasets can be found in their paper.

We implement HRDN using Pytorch1.2 with CUDA 10.1 on NVIDIA Titan RTX GPU. Adam optimizer is used to training the model, we set the weight decay=0.01 to prevent over-fitting. We first train using edge enhanced loss function by set $\alpha = 0.8$ for 20 epoch, the loss quickly decreases to acceptable range. Then we set $\alpha = 1$, so only the L1 Charbonnier loss would be used for fine-tune to achieve higher performance. In

Table 3. Comparative experiments and Quantitative results

	DnCNN	U-net	Sun	MopNet	Our HRDN
PSNR	24.14	27.82	24.07	27.75	28.47
SSIM	0.795	0.860	0.808	0.864	0.860

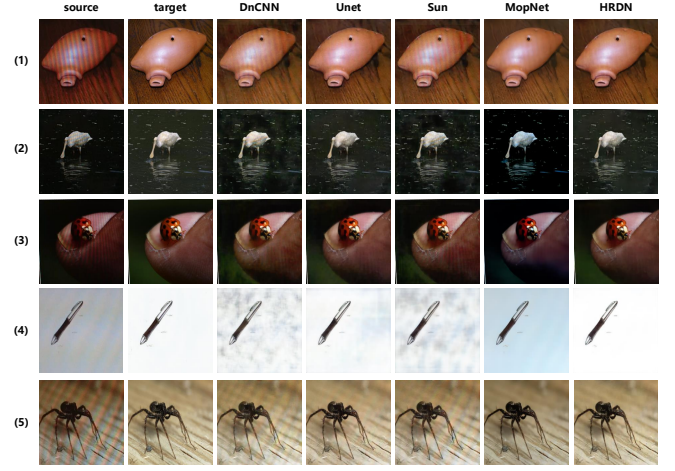


Fig. 5. Qualitative analysis of DnCNN [18], U-net [6], Sun [4], MopNet [1] and our HRDN

our experiments, image size is 256×256 , and batchsize is set to 32. The initial learning rate is $1e-4$, and the learning rate decay is set to 0.5 when loss not decreases or every 10 epoch, we total trained 100 epochs.

4.2. Results

We compare our HRDN with some deep learning based demoiré methods and image restoration methods, such as DnCNN [18] for image denoising, U-net [6], Sun's network [4], MopNet [1]. For a fair comparison, we use Moire Photo Benchmark to retrain all above methods, and compare them on the same testing set. The Peak signal to noise ratio (PSNR) and Structural Similarity (SSIM) are used to evaluate the performance of these methods. All quantitative results are shown in Table 3. It proves that our HRDN is better than other state-of-arts in PSNR and comparable in SSIM.

More specifically, the MopNet [1] use a very complex network structure with the integration of two additional pre-trained networks, which are responsible for predicting the clean edge and classifying moiré pattern to three joint-class, respectively. Different from it, our proposed HRDN is an end-to-end method, and the edge enhanced loss can achieve the same effect as the edge prediction network of MopNet, so our architecture is simpler than MopNet.

We also implement the visual comparison with state-of-arts. The results can be found in Figure 5. Zoom in to get a

better view. From left to right are the moiré image, results of DnCNN [18], U-net [6], Sun’s network [4], MopNet [1] and our proposed HRDN. As shown as in figure, both DnCNN and Sun’s network can not remove moiré pattern successfully, the limitation of MopNet are over-smoothing and inaccurate colors. Our HRDN can get clean demoiré images with better visual effects. By the way, the performance of U-net [6] exceeded our expectations.

4.3. Ablation Study

We also implement some ablation studies for exploring the importance of different part within our HRDN. Three ablation studies were adopted: (1) remove Sobel Loss from full HRDN: rm_SLoss, (2) remove Final Feature Fusion from full HRDN: rm_FFF, (3) remove fuse layer in each IEM: rm_Fuse. Each ablation study conduct on the same training set and re-train for fair competition.

From the observation of Table 4, we can found the fuse layer in each IEM has the largest effect on demoiring, so fuse layer can really explore the relationship between the different branches. Futhermore, Sobel loss and Final Feature Fusion can not only improve effect, but also accelerate the speed of convergence. In our experiments, the valid psnr of Full HRDN can reach 27 on 19th epoch while other ablation studies reach the same value at more than 50th epoch. It demonstrates that such a network structure is able to handle the characteristics of moiré artifacts.

Table 4. Ablation experiments results

	rm_SLoss	rm_FFF	rm_Fuse	Full HRDN
PSNR	28.13	28.24	26.78	28.47
SSIM	0.850	0.855	0.833	0.860

5. CONCLUSION

Moiré pattern is an unpleasant artifact during shooting the LCD screen by smart-phone or cameras. Based on the characteristics of moiré pattern that are multi-frequency and changing dynamically, we proposed a novel High-Resolution Demoiré Network(HRDN). It includes three vital elements: parallel high-resolution network, continuously information exchange modules and final feature fusion layer. These elements can better separate and remove moiré pattern to get more details. Extensive experiments on benchmark data show that our method outperform the state-of-art. In the future, we believe the effect of such post-processing method is limited, the moiré pattern should be eliminated as much as possible when it appears—on the ISP in cameras, a real end-to-end method should be used.

6. REFERENCES

- [1] Bin He, Ce Wang, Boxin Shi, and Ling-Yu Duan, “Mop moire patterns using mopnet,” in *Proceedings of the IEEE International Conference on Computer Vision*, 2019, pp. 2424–2432.
- [2] Zhouping Wei, Jian Wang, Helen Nichol, Sheldon Wiebe, and Dean Chapman, “A median-gaussian filtering framework for moiré pattern noise removal from x-ray microscopy image,” *Micron*, vol. 43, no. 2-3, pp. 170–176, 2012.
- [3] Fanglei Liu, Jingyu Yang, and Huanjing Yue, “Moiré pattern removal from texture images via low-rank and sparse matrix decomposition,” in *2015 Visual Communications and Image Processing (VCIP)*. IEEE, 2015, pp. 1–4.
- [4] Yujing Sun, Yizhou Yu, and Wenping Wang, “Moiré photo restoration using multiresolution convolutional neural networks,” *IEEE Transactions on Image Processing*, vol. 27, no. 8, pp. 4160–4172, 2018.
- [5] Tianyu Gao, Yanqing Guo, Xin Zheng, Qianyu Wang, and Xiangyang Luo, “Moiré pattern removal with multi-scale feature enhancing network,” in *2019 IEEE International Conference on Multimedia & Expo Workshops (ICMEW)*. IEEE, 2019, pp. 240–245.
- [6] Olaf Ronneberger, Philipp Fischer, and Thomas Brox, “U-net: Convolutional networks for biomedical image segmentation,” in *International Conference on Medical image computing and computer-assisted intervention*. Springer, 2015, pp. 234–241.
- [7] Jingyu Yang, Xue Zhang, Changrui Cai, and Kun Li, “Demoiréing for screen-shot images with multi-channel layer decomposition,” in *2017 IEEE Visual Communications and Image Processing (VCIP)*. IEEE, 2017, pp. 1–4.
- [8] Jia Deng, Wei Dong, Richard Socher, Li-Jia Li, Kai Li, and Li Fei-Fei, “Imagenet: A large-scale hierarchical image database,” in *2009 IEEE conference on computer vision and pattern recognition*. Ieee, 2009, pp. 248–255.
- [9] Bolin Liu, Xiao Shu, and Xiaolin Wu, “Demoiréing of camera-captured screen images using deep convolutional neural network,” *arXiv preprint arXiv:1804.03809*, 2018.
- [10] Ke Sun, Bin Xiao, Dong Liu, and Jingdong Wang, “Deep high-resolution representation learning for human pose estimation,” *arXiv preprint arXiv:1902.09212*, 2019.

- [11] Kaiming He, Xiangyu Zhang, Shaoqing Ren, and Jian Sun, “Deep residual learning for image recognition,” in *Proceedings of the IEEE conference on computer vision and pattern recognition*, 2016, pp. 770–778.
- [12] Jonathan Long, Evan Shelhamer, and Trevor Darrell, “Fully convolutional networks for semantic segmentation,” in *Proceedings of the IEEE conference on computer vision and pattern recognition*, 2015, pp. 3431–3440.
- [13] Alejandro Newell, Kaiyu Yang, and Jia Deng, “Stacked hourglass networks for human pose estimation,” in *European conference on computer vision*. Springer, 2016, pp. 483–499.
- [14] Yilun Chen, Zhicheng Wang, Yuxiang Peng, Zhiqiang Zhang, Gang Yu, and Jian Sun, “Cascaded pyramid network for multi-person pose estimation,” in *Proceedings of the IEEE Conference on Computer Vision and Pattern Recognition*, 2018, pp. 7103–7112.
- [15] Jiwon Kim, Jung Kwon Lee, and Kyoung Mu Lee, “Accurate image super-resolution using very deep convolutional networks,” in *Proceedings of the IEEE conference on computer vision and pattern recognition*, 2016, pp. 1646–1654.
- [16] Wenzhe Shi, Jose Caballero, Ferenc Huszár, Johannes Totz, Andrew P Aitken, Rob Bishop, Daniel Rueckert, and Zehan Wang, “Real-time single image and video super-resolution using an efficient sub-pixel convolutional neural network,” in *Proceedings of the IEEE conference on computer vision and pattern recognition*, 2016, pp. 1874–1883.
- [17] Jie Hu, Li Shen, and Gang Sun, “Squeeze-and-excitation networks,” in *Proceedings of the IEEE conference on computer vision and pattern recognition*, 2018, pp. 7132–7141.
- [18] Kai Zhang, Wangmeng Zuo, Yunjin Chen, Deyu Meng, and Lei Zhang, “Beyond a gaussian denoiser: Residual learning of deep cnn for image denoising,” *IEEE Transactions on Image Processing*, vol. 26, no. 7, pp. 3142–3155, 2017.